**Important Notice to Authors**

Attached is a PDF proof of your forthcoming article in *Journal of Nanophotonics*.

***No further publication processing will occur until we receive your response to this proof. Please respond within 48 hours of receipt of this message.***

**Questions & Comments to Address**

Please see the back page of this PDF proof for an itemized list of questions and comments to be addressed. The numbers listed correspond to numbers in the margin of the proof pages pinpointing the source of the question and/or comment. The numbers will be removed from the margins prior to publication.

**Other Items to Check**

- Please check your title, author list, and acknowledgments carefully for any omissions or errors. Also check all text, illustrations, captions, equations, tables, references, and author biographies thoroughly. If you are adding biographies, note that they should not exceed 75 words each. Authors are encouraged to upload photographs and update their online SPIE profile on our website at http://spie.org/app/profiles/default.aspx.
- Please proofread the article very carefully. This will be your only opportunity to provide corrections. Note that responsibility for detecting errors lies with the author.
- Please check that your figures are accurate and sized properly. Figure quality in this proof is representative of the quality to be used in the online journal. To achieve manageable file size for online delivery, some compression and downsampling of figures may have occurred. Fine details may have become somewhat fuzzy, especially in color figures. The print journal uses files of higher resolution and therefore details may be sharper in print.

**Ways to Respond**

- Web: If you accessed this proof online, follow the instructions on the web page to submit corrections.
- Email: Send corrections to spie-manager@luminad.com. Include the paper number for your article in the subject line.

**Forms**

*Journal of Nanophotonics* offers the option of open access publication for a flat fee of $960 ($660 for Letters). Open access papers will be published under a Creative Commons CC BY 3.0 license. Authors who do not pay for open access will be published under the standard SPIE Transfer of Copyright agreement.

- Pay the open access fee online at http://spie.org/publications/journals/pubcharges.
- If you haven't already, complete the appropriate publication license online by logging into your account at http://jnp.msubmit.net.

**If You Need to Contact Us**

You may send an email message to spie-manager@luminad.com. Please reference the paper number and the first author of your article in your subject line. We will respond to you via email as quickly as possible.

# Metal-enhanced fluorescence emission and quenching protection effect with a host–guest nanophotonic-supramolecular structure

**Alicia V. Veglia[a] and Angel Guillermo Bracamonte[a,b,*]**

[a]Universidad Nacional de Córdoba, Ciudad Universitaria, Instituto de Investigaciones en Físico Química de Córdoba, Departamento de Química Orgánica, Facultad de Ciencias Químicas, Córdoba, Argentina

[b]Université Laval, Departement de Chimie and Centre d'optique, photonique et laser, Québec, Canada

**Abstract.** The functionalization of the nanoparticle's (NP) surface is one method for tuning their overall properties to fit targeted applications. We developed a nanosensor based on the specific supramolecular interactions between **ß**-cyclodextrin (**ßCD**) nanocavities and organic molecules of biological interests using the metal-enhanced fluorescence effect (**MEF**) as the detection signal. We grafted **ßCD**, a typical macrocyclic host molecule that interacts specifically with different organic molecules and changes their physical properties (such as their fluorescence emission intensity), on gold NPs. To evaluate this nanosensor and the effect of the metallic core, we worked with a typical organic molecule, Rhodamine B (**RhB**), that has a strong association constant with **ßCD** (5700 $M^{-1}$) and is well-known to be quenched in the presence of cyclodextrins (CDs). The results show that, by grafting **ßCD** on gold NPs, it is possible to increase the sensitivity of **RhB** detection by 70%, 80%, and 294% when compared with solutions in (1) a phosphate buffer, (2) with **ßCD**, and (3) with Au NPs, respectively. These results show that the use of a supramolecular system attached to a metallic NP can interact specifically with a dye to enhance its fluorescence emission through the MEF effect. Moreover, this type of nanosystem can overcome the quenching of the signal by the matrix, such in the case of **RhB** with CDs. Eventually, this concept could be extended to other dyes with different quenching effects. For this reason, this type of nanosensor system could be used in the future to protect and enhance the dye emission of fluorophores in different biological media.  [DOI: 10.1117/1.JNP.12.3.XXXXXX]

**Keywords:** gold nanoparticles; quenching protection; metal-enhanced fluorescence; enhanced sensitivity; nanophotonic-supramolecular systems.

Paper 18013SSP received Jan. 17, 2018; accepted for publication Apr. 25, 2018.

## 1 Introduction

Supramolecular chemistry is the chemistry of noncovalent interactions defined by Lehn that permits different types of complexes targeting molecular interactions; as such, it is an interesting field that is in continuous development[1] for multiple designs of nanoarchitectures[2] and applications.[3,4] From these interactions, the physicochemical properties of the molecule are complex and modify their solubility and the spectroscopic properties. These changes can be used in different applications that emulate antigen–antibodies interactions. Within this field, many developments related to emerging tools in biotechnology based on **MEF** applying antigen–antibodies recognition for nanostructures surface designs[5] for ultrasensitive fluorescence sensing assay platforms[6] are in progress. Additionally, from supramolecular chemistry in the last few

*Address all correspondence to: Angel Guillermo Bracamonte, E-mail: gbracamonte@fcq.unc.edu.ar

1934-2608/2018/$25.00 

years, new nanoarchitectures based on nanoparticles (NPs) grafting with natural and synthetics supramolecular systems have been developed. For example, Chen et al.[7] developed a nanosensor with silver NPs grafted with **ß**-cyclodextrin (**ßCD**) nanocavities as a supramolecular system for the spectrophotometry enantiomeric discrimination of phenolic compounds.

**CDs** are cyclic oligosaccharides consisting of six (**αCD**), seven (**ßCD**), or eight (**γCD**) units of $\alpha$–D-glucose linked by $\alpha$-(1, 4) bonds. These macrocycles have a nanocavity (internal diameter of 0.7 nm for **βCD**) that allows them to act as hosts to form inclusion complexes with guest molecules in the solid state or in solution.[8] The CDs are interesting microvessels capable of embedding appropriately sized molecules, and the resulting supramolecules can serve as excellent miniature models for enzymes–substrates complexes.

Moreover, Brouard et al.[9] designed an DeoxyriboNucleic Acid sensing architecture combining the molecular recognition capabilities of a cationic conjugated polymer transducer with highly fluorescent core–shell NPs exploiting metal-enhanced fluorescence (**MEF**). **MEF** is an effect produced by the interaction of fluorophores (at a specific distance from the metallic surface) with metallic NPs plasmon that increases the electronic occupancy of the fluorophore-excited state.[10] Then, Bracamonte et al.[11] developed a nanosupramolecular complex for switch *on/off* enhanced fluorescence control and molecular release using a simple chemistry reaction based on molecular recognition coupled to **MEF**.

These types of research works open the possibility to explore **MEF** as a detection signal in new analytical methodologies using nanosupramolecular sensors looking to improve analytical performances of the supramolecular systems.

For this reason, we propose exploring the designing of nanosensors joining the knowledge of supramolecular systems with metallic NPs based on nanoimaging and single NP analysis with potential applications in nanophotonics and single molecular detection.

Rhodamine B (**RhB**) is an important xanthene dye with a large variety of technical applications, such as dye lasers, photosensitizer, and quantum counter, etc.[12] The spectroscopic and photophysical properties of **RhB** has been extensively studied in different media. A recent example is by Zhu et al. who studied the mechanisms of interaction between bovine serum albumin with **RhB** using fluorescence spectroscopy. Moreover, it is well-known[13,14] that **RhB** interacts strongly with **βCD** accompanied by a quenching effect.[15]

Based on our previous research work applying PEG molecules as spacer and linkers of supramolecular systems,[11] it obtained excellent properties as well dispersible NPs, molecular recognition, controlled switch on-off enhanced fluorescence detection, and no cell adsorption properties. However, for photonics applications, a higher density and more compact nanoarchitecture should be developed. For this reason, this research work was related to the synthesis of plasmonic gold core **βCD** grafted by applying a compact short conjugated organic molecular spacer shell. In this manner, their plasmonic properties were evaluated for **MEF** applications.

## 2 Experimental

### 2.1 *Apparatus*

UV–vis and spectrofluorimetric determinations were carried out in a Varian UV-50 Carry 50 Conc. and a Fluorolog HORIBA JOBIN YVON, respectively. The lifetime measurements were done with a Fluotime 2000. The pH was measured with a Fisher Scientific Accumet model Excel XL20 at $(25.0 \pm 0.1)$°C. The pH meter was first calibrated using standard buffers (pH = 4.00, 7.00, and 9.00). An ultrasonic bath (Branson 2510) was used for the dispersion of the reagents. The transmission electron microscopy (TEM) images were taken using a TEM JEM-1230, JEOL with an operating voltage of 200 kV. Data analysis was performed with Origin (Scientific Graph system) version 8.

### 2.2 *Reagents*

The water was obtained using a Millipore apparatus. **RhB** (99% purity, Sigma-Aldrich), **βCD** (98% purity, Sigma), hydrogen tetrachloroaurate, $HAuCl_4.3H_2O$ (99%, Sigma-Aldrich), citrate

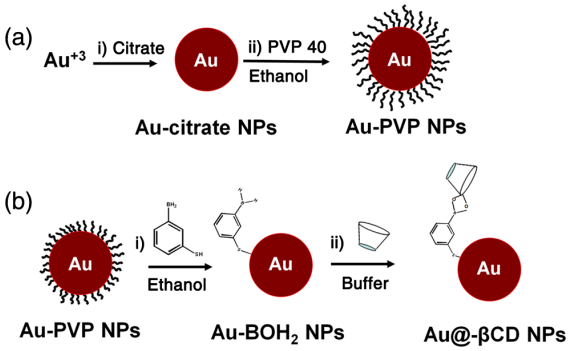


**Fig. 1** Schematic representation of the synthesis: (a) gold NPs synthesis and (b) **βCD** grafting of gold NPs.

sodium tribasic dihydrate (99%, ACS reagent), polyvinyl pyrrolidone 40 000 g/mol (98%, Sigma-Aldrich), and mercaptophenylboronic acid (≥95%, Aldrich) were used as received. The pH = 7.4 (10 mM) buffer was prepared according to literature procedures (2.3 mM monosodium dihydrogenphosphate and 7.7 mM disodium hydrogenphosphate). All constituents of the buffers were commercial reagents of analytical grade.

### 2.3 *General Procedure*

A concentrated aqueous solution of **RhB** 0.626 mM (3 mg/10 mL) was stored in the refrigerator (4°C) for a maximum of 20 days. The stability of the stock solutions was periodically checked by spectrophotometry before preparing the appropriate dilutions for fluorimetric determinations. All the experiments were done with diluted aqueous solutions of **RhB** in the nM range to ensure only the monomeric specie was present.[15] All the solutions were covered with aluminum foil to protect them from light exposure. For emission and excitation fluorescence spectra, the excitation and emission bandwidths were set at 5 nm. The fluorescence emission spectra were measured with an excitation wavelength equal to the wavelength of maximum absorption (540 nm). All the measurements were made at $(25.0 \pm 0.1)$°C, with the temperature of the cell compartment controlled with a Haake K10 circulator with continuous stirring.

The gold NPs were synthesized by the classical Turkevich method of citrate reduction of $HAuCl_4$ and were afterward stabilized with PVP 40. The resulting NPs were then redispersed in anhydrous ethanol (mother solution, [Au NPs] $= 388 \times 10^{10}$ NPs/mL, diameter = 55.5 nm).

The grafting of **βCD** on the gold NPs was done by mixing 2 mL of the ethanolic NPs solution capped with PVP 40 with a 5 mM ethanolic solution of mercaptophenylboronic acid for 3 h with continuous agitation. Afterward, the NPs were redispersed in a phosphate buffer (10 mM, pH 7.40). The resulting NPs were mixed with 2 mL of a 10 mM **βCD** phosphate buffer solution for 2 h to covalently bind the **βCD** (Au@**βCD**) to the boronic acid monolayer (see synthesis Fig. 1).

The sensitivities and lifetime measurements of the **RhB** were measured for different media (Au@**βCD**, the buffer solution, free **βCD**, free Au NPs, and a mechanical mix of free **βCD** and free Au NPs). Low concentrations ($\sim 3.88 \times 10^8$ NPs/mL or a dilution factor of 100 of the initial gold mother solution) of gold NPs were used to avoid autoabsorption (extinction coefficient inferior to 0.05). The CDs concentrations were between milli- and micromolar. The mechanical mix was done with the simple addition of NPs capped with PVP 40 and **βCD** without the addition of any linker.

## 3 Results and Discussion

### 3.1 *Nanoparticles Characterization*

The gold NPs were synthesized by the classical Turkevich method of citrate reduction of $HAuCl_4$. Particles synthesized by this method were nearly monodisperse spheres, with their

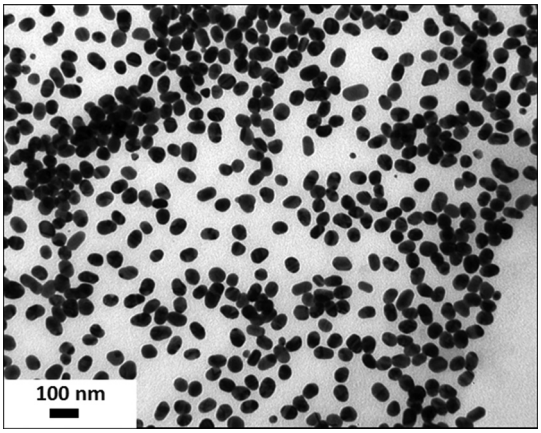


**Fig. 2** TEM of gold NPs synthesized by the classical Turkevich method of citrate reduction of $HAuCl_4$. Monodisperse spherical gold NPs of 55.5-nm diameter were obtained.

sizes easily controlled by the initial reagent concentrations ratios. We synthesized monodisperse spherical gold NPs in the 40- to 50-nm-diameter range for our work (Fig. 2).

They are easily characterized in UV by their plasmon absorbance band centered around 540 nm for the 55.5-nm gold NPs (Fig. 3). Surface modifications of the Au NPs (Fig. 4) can easily be observed in UV. For instance, the grafting of the boronic linker can be evidenced with the apparition of a band at 250 nm. Furthermore, the grafting of organic molecules on the

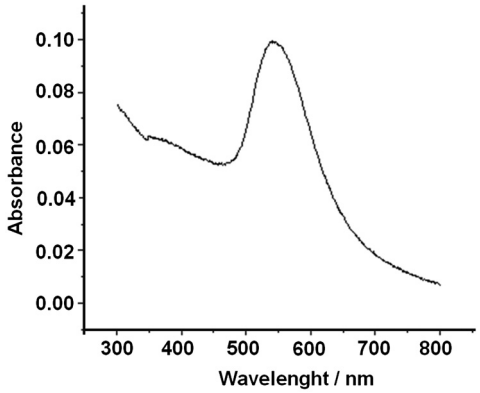


**Fig. 3** UV spectra of gold NPs in buffer phosphate pH = 7.40 (diameter = 55.5 nm), NPs stabilized with citrate.

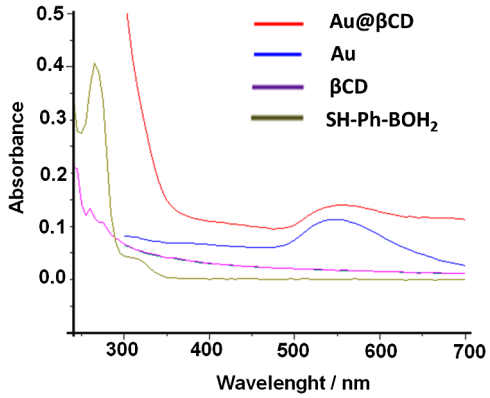


**Fig. 4** UV spectra comparison of gold NPs (PVP-40 stabilized) with gold NPs **βCD** grafted.

gold surfaces redshifts the plasmon band by a few nanometers. We also observed the apparition of a third band at 650 nm, attributed to **βCD** grafting on gold NPs. It is consistent with results reported in previous publications, where modified CDs (such as pyridylmethyl-amino-$\beta$-cyclodextrin) were grafted on gold NPs.[16]

### 3.2 *Study of the Rhodamine B Fluorescence Effect in Presence of β-Cyclodextrin Gold Nanosensor*

We monitored changes over a 1-h period in the fluorescence spectra of Au@**βCD** in the presence of 1.00 nM of **RhB** with continuous stirring. As seen Fig. 5, there is an increase of the **RhB** emission signal ($\lambda_{max.\,em.}$ 580.0 nm), accompanied by a 6-nm blueshift in the emission peak wavelength over the first 45 min, after which it stabilizes. Another band of the CDs emission signal was observed with the time around ($\lambda_{max.\,em.}$ 520.0 nm) but without a shift in the wavelength emission. The deconvolution of the spectra in two Gaussian bands and the subtraction of the 520.0 nm band to the 580.0 nm band assigned to the **RhB** emission gives a result of a net emission increment.

These effects can be explained by the high-electron density prevailing inside the **βCD** cavity, which can mobilize the electrons of the included guest molecule,[17] thus resulting in changes in the spectral properties of both the guest and the **βCD** itself. Moreover, these observations are related not only to the specific interactions between the dye and the **βCD** nanocavity but to the time needed to get all the system in equilibrium to obtain a constant emission fluorescence signal. The system in total equilibrium is not only related to the time of a simple host–guest interaction (typically Van der Walls attractions between the **RhB** and the **βCD** nanocavity) but also through H-bonding between several CDs moietie's hydroxyl groups. We believe the bulk of these interactions occurs between CDs grafted over different NPs, although interactions between these macrocycles grafted over the same gold surface have been demonstrated before.[18,19] Initial inclusion of the guest in the cavity is very rapid (often within minutes), but the final equilibrium can take much longer to reach. Once inside the CD cavity, the guest molecule undergoes conformational adjustments to take maximum advantage of the weak van der Waals forces that exist.[20] Another factor to consider for the stabilization of the fluorescence signal is the homogenization of the nanosupramolecular system, which takes into account the movement of the NPs and the interactions between their surface's moieties.

In these conditions, we also observed, over 50 min, a gradual increase of about 36% to 40% of the **RhB** emission in the presence of Au@**βCD**. This is a high increase considering that, at best, there is a 0.5 nM concentration of **βCD** over the gold NP's surface. Comparing this value with results in literature, we found that, to measure a fluorescent increment of **RhB** in the presence of **βCD**, it is necessary to work at higher concentrations of dye and **βCD** (dye $\sim 10^{-3}$ M and

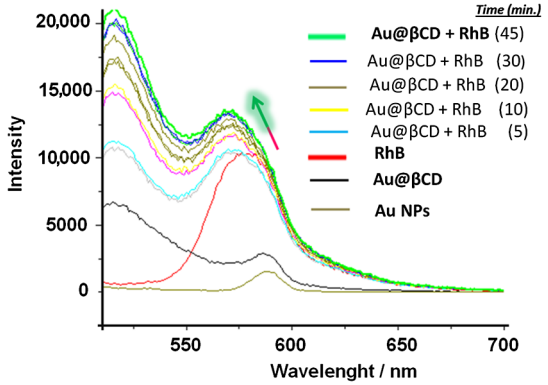


**Fig. 5** Fluorescence emission of **RhB** in different media and their blanks: the green line emission corresponded to Au@**βCD** after the stabilization time of around 45 min ($\lambda_{max.\,em.} = 574.0$ nm), red line to **RhB** emission, ($\lambda_{max.\,em.} = 580.0$ nm), black line to Au@**βCD** blanks, and brown line to Au NPs blank with $H_2O$ Raman $\lambda = 588.0$ nm. The excitation wavelength was 540.0 nm.

**βCD** 10 mM) than in our experimental conditions (nM concentrations of host and guest). At lower **RhB** concentrations, in the ($10^{-4}$ to $10^{-8}$) M range, quenching was measured.

To our knowledge, there are no reported studies claiming that such concentrations are able to enhance the fluorescence emission of **RhB** or any other dye at such an extent. Indeed, most studies pertaining to the inclusion of organic compounds in CDs use macrocycles concentrations in the mM range;[21] in these conditions, there is a high inclusion percentage of the dye into de-CDs cavity.

The CDs cavity behaves like an organic solvent, notably oxygenated solvents, such as dioxane, tert-amyl alcohol, and 1-octanol,[22] as it contains an oxygen atom while affording an apolar surrounding to the guest allowing fluorescence emission changes. It is known that **RhB** emission is quenched by the addition of **βCD**. In this manner, it was showed the characteristic quenching effect of **βCD** (10 mM) on the **RhB** fluorescence emission (the quenching effect measured was ~25%) (Fig. 6), as well as the same characteristic blueshift ($\lambda_{max.\,em.}$ 574.0 nm), was observed for this dye in literature.[23]

Moreover, we compared the effect of the Au@**βCD** on the **RhB** emission with gold NPs stabilized with PVP 40 (Fig. 7). There is a 30% diminution of the **RhB** emission. This effect could be explained by a nonspecific adsorption effect of **RhB** over the metallic NP surface. In this case, it is known that a quenching effect appears through a nonradiative energy transfer to the

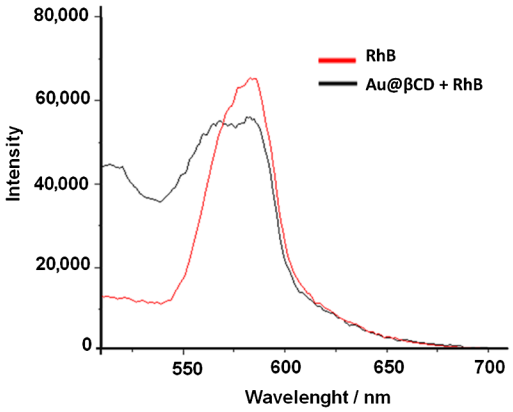


**Fig. 6** Fluorescence spectra of **RhB**: in buffer phosphate pH = 7.40 (red line) ($\lambda_{max.\,em.}$ = 580.0 nm) and in **βCD** (black line) ($\lambda_{max.\,em.}$ = 574.0 nm). The **RhB** and **βCD** concentrations were 1.0 nM and 10.0 mM, respectively.

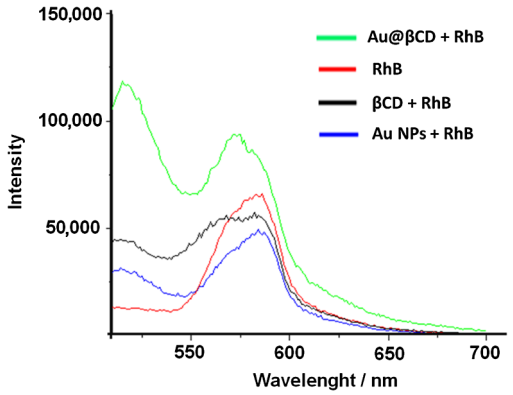


**Fig. 7** Comparison of fluorescence emission of **RhB** in different media: green line corresponded to Au@**βCD** ($\lambda_{max.\,em.}$ = 574.0 nm), red line in buffer ($\lambda_{max.\,em.}$ = 580.0 nm), black line in βCD ($\lambda_{max.\,em.}$ = 574.0 nm), and blue line for Au NPs ($\lambda_{max.\,em.}$ = 580.0 nm). The excitation wavelength was 540.0 nm.

metal surface when the fluorophore is too close to the metallic surface.[24] Or another possible explanation is the diminution of emission caused by inner filter effect.

Thus, without **βCD** linked to the NP that is in the presence of gold NPs without any type of specific supramolecular interactions, it was not possible to obtain an enhanced fluorescence signal similar to the one obtained with the nanosensor Au@**βCD**. For this reason, we interpreted the **RhB** emission increment observed in the presence of Au@**βCD** not only as a consequence of the inclusion complex formed between the **βCD** and **RhB** but to the proximity of this complex to the metallic surface, which results in **MEF**. While this increment might not seem high when compared with other reported results with metallic core–shell NPs modified with fluorophores, we have to take into account the low percentage of **RhB** that is incorporated over the surface. In metallic core-silica shell NPs, it is possible to add fluorophore concentrations in the order of $\mu$M due to the possibility of tuning the fluorescent silica shell; while for similar NPs concentrations of Au@**βCD** NPs, it is possible just to incorporate in the nM concentration range based on the total number of **βCD** attached per NP. So, such results in the presence of low **RhB** concentration level showed the powerful interaction between the dye and **βCD** complex and the gold NP. Moreover, it is well-known that **MEF** is related to the distance between the metal surface and the fluorophores. Different studies of the metal–fluorophore interaction show this dependence. Wokaun et al.[25] reported a maximum luminescence enhancement of 200 for a 25-Å-thick evaporated layer of $SiO_2$ on a planar silver island film. Moreover, we studied this phenomenon with a multilayered nanoarchitecture that features a metal core surrounded by concentric silica layers containing FRET donor and acceptor molecules. We demonstrated the importance of the precise distance between these molecules and the core,[26] as well as this effect by applying flexible and short PEG molecular spacers.[11]

While the spacer's length, here, is not optimal, considering that it is at most, around 19 Å (considering 4 Å for the linker and 15 Å for the **βCD**), the system has a sufficient spacer (Fig. 8) to permit **MEF**, based on a higher density of the molecular spacer that places the fluorophore at a given distance by a supramolecular interaction (Fig. 9) diminishing in this manner the incorporation of free dyes close to the gold surface accompanied with a quenching effect.

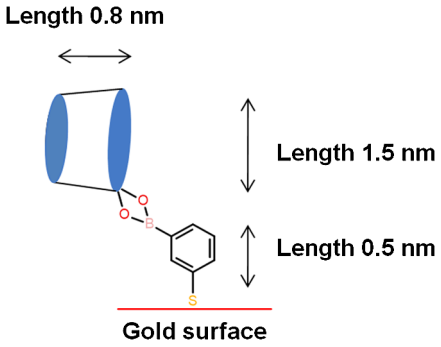


**Fig. 8** Schematic representation of the supramolecular system linked over the gold surface with approximate dimension.

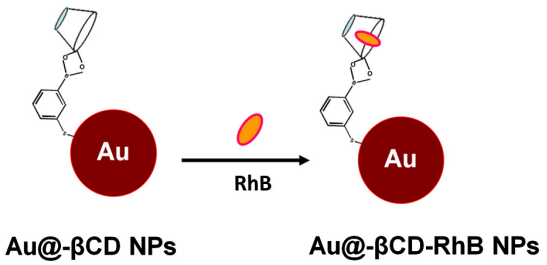


**Fig. 9** Molecular recognition event based on a supramolecular interaction and plasmonic interaction.

On the basis of these results and to evaluate this nanosensor based on a molecular recognition coupled to a Plasmonic effect, we made a calibration curve for **RhB** in different media: (1) Au@**βCD**, (2) free **βCD**, (3) free Au NPs mixed with free **βCD** (nongrafted), (4) free Au NPs in a pH 7.30 phosphate buffer solution, and (5) the same buffer (Fig. 10).

The analytical parameters are summarized in Table 1. The calibration curves show the higher sensitivity when in the presence of the nanosensor compared with all the other media tested. Comparing the performances between the Au@**βCD** system and the systems with free Au NPs and **βCD**, we see an increment of the sensitivity by 294% and 70%, respectively. As mentioned, this increase stems from the **MEF** effect between the gold core and the probed fluorophores. Moreover, the sensitivity in the buffer is 45% higher than in the presence of **βCD**, which shows the quenching effect of this macrocycle on the **RhB** emission. In the case of the mechanical mix, with different **βCD** concentrations (between milli- and micromolar), the sensitivities were similar to or smaller than the one obtained in the buffer.

The guest's fluorescence in the presence of free **βCD** is expected to be quenched; however, the **MEF** resulting from the **βCD** complex nearby metallic surface results in a net increase in the fluorescence signal, but this observation is measured only in the case that the **βCD** is attached to the metallic NP surface. With the mechanical mix, composed by free NPs with **βCD** added in absence of linker, it was not observed an increment in the sensitivity value (in comparison with buffer and **βCD**) showing the well-known importance of the distance fluorophore-metallic NP dependence.

In our best knowledge, there are not many publications related to this field that compare different molecular spacers to design nanosensors using gold NPs in colloidal dispersion. Moreover, there are many publications for **MEF** studies based on metallic surfaces and

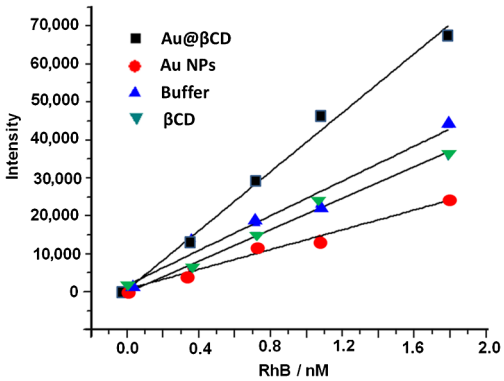


**Fig. 10** Comparison of **RhB** calibration curves in the presence of different media. All the measurements were done in buffer phosphate pH = 7.40. The Au@**βCD** and Au NP concentrations were the same and estimated by UV measurements. The **βCD** concentration was 10 mM. The fluorescence intensity was taken at the maximal emission wavelengths of each media.

**Table 1** Sensitivities values of **RhB** in different media.

| System[a] | m[b]/10[3] | Adjacent $R^2$ |
|---|---|---|
| Au@**βCD**[c] + **RhB** | 39 ± 2 | 0.993 |
| Au NPs[c] + **RhB** | 13 ± 1 | 0.994 |
| Buffer+ **RhB** | 23 ± 2 | 0.978 |
| **βCD** + **RhB** | 21 ± 1 | 0.992 |

[a]All the measurements were done in water buffer phosphate solution pH = 7.40 solution.
[b]Slope of the calibration curve from lineal equation $y = a + b * x$.
[c]UV spectra were measured of the NP sample to have similar NP concentration.

polymeric spacers showing the enhanced effect; however, not many are related to molecular sensing at low concentration levels. Comparing the methodologies proposed by applying CDs as molecular receptor, the concentrations used are higher in the $\mu$M level, while in the presence of nM, none were reported (these Au@**βCD** NPs contain the best 50 nM of CDs grafted in concentrated NP conditions).

For these reasons, this nanosystem is a proof of concept to be applied for molecular tracking, single molecule detection with biological interest accompanied with more analytical advantages and performances than only using supramolecular systems. These NPs functioned as nanoplatforms for molecular trapping detection by an enhanced fluorescence detection based on a supramolecular interactions coupled to MEF.

### 3.3 *Lifetimes Measurements*

To understand the photophysics of the **RhB** and to obtain more direct information about the microenvironmental changes around the fluorophore interacting with the different media, we measured the lifetimes in the conditions described before. The fluorescence lifetime decay curves (Fig. 11) showed a shortening of **RhB** lifetimes decays in the presence of the nanosensor (Fig. 12) with respect to the free **RhB** in buffer phosphate and in the presence of free gold NPs (without the **βCD** grafted). All the results are shown in Table 2.

The lifetimes obtained for **RhB** in buffer were 1.6 ns, which agrees with the results reported earlier (1.6 ns)[27] and (1.7 ns).[28] In the presence of free gold NPs, a similar value was obtained, showing that a diminution effect in the lifetime is needed to have a specific supramolecular molecular recognition. In the case of the nanosensor, the curve was fitted for two lifetimes decay;

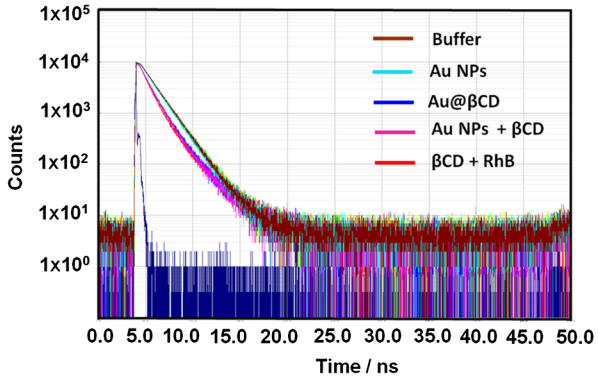


**Fig. 11** Fluorescence lifetime decays of **RhB** in different media.

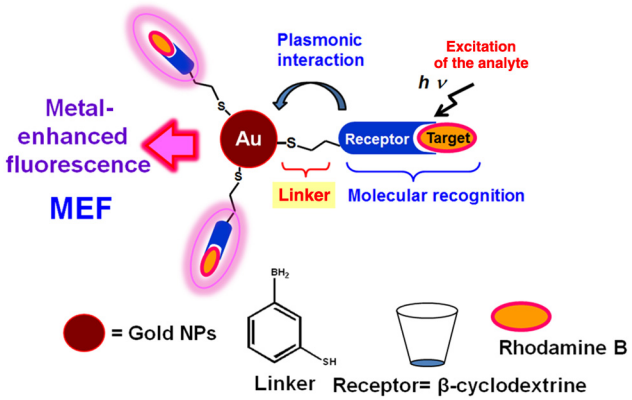


**Fig. 12** Schematic representation of a gold nanosupramolecular system formed by the gold core (red circle), the linker corresponded to mercaptophenylboronic acid, the receptor of **βCD** (truncated cone) and Rhodamine B (orange oval).

**Table 2** Fluorescence decay parameters of **RhB** in different media.

| System + **RhB** | | $\tau_1$ (ns) | | $\tau_2$ (ns) | | $\tau_{average}$ (ns) | $\chi^2$ |
|---|---|---|---|---|---|---|---|
| | | Value | Area | Value | Area | | |
| Buffer | | 1.64 ± 0.04 | 12392 | — | — | 1.641 | 1.009 |
| Au NPs | | 1.62 ± 0.01 | 12338 | — | — | 1.621 | 1.002 |
| Au@**βCD** | | 1.92 ± 0.07 | 3672 | 0.90 ± 0.04 | 9070 | 1.185 | 1.001 |
| **βCD** + **RhB** | | 2.24 ± 0.09 | — | 0.93 ± 0.03 | — | 1.108 | 1.004 |
| Au NPs + **βCD** | 10 mM | 1.90 ± 0.08 | 3375 | 0.88 ± 0.03 | 9560 | 1.159 | 1.005 |
| | 0.1 mM | 1.58 ± 0.01 | 12660 | — | — | 1.582 | 1.159 |
| | 0.001 mM | 1.62 ± 0.01 | 12445 | — | — | 1.625 | 0.998 |

the first can be interpreted as **RhB** included in the **βCD** nanocavity (0.90 ns) corresponding to the fluorophore next to the metallic surface with **MEF**, and the second is the free **RhB** (1.92 ns) with a higher $\tau_i$ due to the fluorophore sensing an other more apolar environment. Moreover, the average decay of the nanosensor (1.18 ns) is smaller than the one for free **RhB** in buffer and in the presence of gold NPs (1.6 ns). Due to this, the $\tau_i$ value in the presence of gold NPs and in buffer are similar, the fluorescence diminution in the presence of gold NPs is explicated by an inner filter effect. The enhanced signal of fluorescence emission is known to be accompanied by a diminution of the lifetime in the excited state.[29,30] In our working experimental conditions, it is important to know that the lifetime diminution is caused by a supramolecular molecular recognition with a total theatrical **βCD** concentration over NP surface at the best, around 0.5 nM.

With the results obtained by mechanical mix, we can see an effect with the **βCD** concentration added; at high concentration (∼10.0 mM), we can see the first lifetime decay related at the **βCD** quenching effect (0.9 ns) and the second lifetime decay higher (1.90 ns). Both values are affected by a media change, such as organized systems as micelles, vesicles, etc., caused by the high **βCD** concentration and interaction intermacrocycles by a network of hydrogen bonds.[31] At high **βCD** concentration, it is possible to obtain CDs aggregation with micellar-like structures,[32] and especially with high stability in comparison with the other CDs.[33] In addition to this concept, it is well-known that **RhB** shows a higher lifetime in an adsorbed state than in aqueous solution because the internal rotation of the diethyl amino group, which is believed to play the main role in the radiation less decay of this molecule, is suppressed under adsorption.[34] In the experiments done, in the mechanical mix at higher **βCD** concentration or with free **βCD** (10.0 mM), generated aggregates and **RhB** adsorbed that produced an increment in the Fluorescent Lifetime Decays accompanied with a deactivation of the excited state as well.

In the presence of smaller **βCD** concentrations, the micellar effect disappeared and we obtained only the lifetime decay of free **RhB**, due to the **βCD** quenching effect over the **RhB** emission always being observed at a high ratio of **βCD/RhB** concentrations.[35] Similar values (2.24 and 0.93 ns) related to similar effects of with the mechanical mix were measured in the presence of only **βCD** (∼10.0 mM).

Comparing the case of mechanical mix with the higher **βCD** concentration and the nanosensor, we can see similar results in the lifetime measurements but not in the sensitivities values, showing the functionality of the nanosensor based on a molecular recognition accompanied with **MEF** detection, which any mechanical mix could reproduce.

In conclusion, with any mechanical mix, we did not obtain the same results (by lifetime measurements and sensitivity determinations) as with the nanosensor (with the **βCD** linked to the gold NP surface and the specific supramolecular guest interaction) probing the effectiveness of the supramolecular host–guest interaction and MEF effect.

## 4 Conclusion and Outlook

To conclude, in our work, we were able to synthesize a nanosystem with the knowledge of the supramolecular chemistry coupled to metallic gold NPs exploiting **MEF** phenomena. Better sensitivities were obtained with the nanosupramolecular system than with supramolecular system only. It was possible to increase the sensitivity of **RhB** detection by 70%, 80%, and 294% when compared with a solution in a phosphate buffer, with free **ßCD**, and with Au NPs, respectively. Further studies of this nanosupramolecular system approach will be developed to obtain higher sensitivities and selectivities for biomolecule detection.

## Acknowledgments

We would like to gratefully acknowledge the different grants received to accomplish the research work in progress in this field: CONICET, Consejo Nacional de Investigaciones Científicas y Técnicas (National Research Council of Argentine); ANPCyT, Agencia Nacional de Promoción Científica y Tecnológica (National Agency of Scientific and Technology Promotion of Argentine); and especially to SECyT (Secretary of Science and Technology from the National University of Cordoba, Argentine, for awarding us the extension of the grant for young researchers. Moreover, special thanks to Professor Denis Boudreau from the Département de chimie and Centre d'optique, photonique et laser, Québec, Canada, for the collaboration in the research work in progress as well as special thanks to all the Canadian Grants, Natural Sciences and Engineering Research Council of Canada (NSERC) and Fonds de recherche du Québec-Nature et technologies (FRQNT), that permitted to accomplish this research work. Finally, special thanks to Rosalia F. Bracamonte for the English revision.

## References

1. E. V. Anslyn, "Supramolecular analytical chemistry," *J. Org. Chem.* **72**, 687–699 (2007).
2. M. W. Ambrogio et al., "Snap-top nanocarriers," *Org. Lett.* **12**(15), 3304–3307 (2010).
3. K. K. Cotí et al., "Mechanised nanoparticles for drug delivery," *Nanoscale* **1**, 16–39 (2009).
4. L. Zhang et al., "A nanomesh scaffold for supramolecular nanowire optoelectronic devices," *Nature Nanotech.* **11**, 900–906 (2016).
5. K. Aslan et al., "Metal-enhanced fluorescence: an emerging tool in biotechnology," *Curr. Opin. Biotechnol.* **16**, 55–62 (2005).
6. Z. Gryczynski et al., "Metal-enhanced fluorescence: a novel approach to ultra-sensitive fluorescence sensing assay platforms," *Proc. SPIE* **5321**, 275–282 (2004).
7. X. Chen et al., "β-cyclodextrin-functionalized silver nanoparticles for the naked eye detection of aromatic isomers," *ACS Nano* **4**, 6387–6394 (2010).
8. M. L. Bender and M. Komiyama, *Cyclodextrin Chemistry*, Springer-Verlag, Berlin, Heidelberg (1978).
9. D. Brouard et al., "Label-free biosensing based on multilayer fluorescent nanocomposites and a cationic polymeric transducer," *ACS Nano* **5**, 1888–1896 (2011).
10. J. R. Lackowicz, "Radiative decay engineering: metal enhanced fluorescence and plasmon emission," *Anal. Biochem.* **337**, 171–194 (2005).
11. A. G. Bracamonte et al., "Nano-supramolecular complex synthesis: switch on/off enhanced fluorescence control and molecular release using a simple chemistry reaction," *Microchem. J.* **128**, 297–304 (2016).
12. M. C. Marchi, S. A. Bilmes, and G. M. Bilmes, "Photophysics of rhodamine B interacting with silver spheroids," *J. Colloid Interface Sci.* **218**, 112–117 (1999).
13. Y. Liu et al., "Unique fluorescence behavior of Rhodamine B upon inclusion complexation with novel bis(beta-cyclodextrin-6-yl) 2, 2'-bipyridine-4, 4'-dicarboxylate," *Org. Lett.* **3**, 1657–1660 (2001).
14. D. Yuan et al., "Synthesis of fullerene-cyclodextrin conjugates," *Tetrahedron Lett.* **42**, 6727–6729 (2001).
15. I. R. Politzer et al., "Effect of $\beta$-cyclodextrin on the fluorescence, absorption and lasing of rhodamine 6G, rhodamine B and fluorescein disodium salt in aqueous solutions," *Chem. Phys. Letter* **159**, 258–262 (1989).

16. Q. Zeng et al., "Host–guest directed assembly of gold nanoparticle arrays," *Langmuir* **26**(2), 1325–1333 (2010).
17. S. Li and W. C. Purdy, "Cyclodextrins and their applications in analytical chemistry," *Chem. Rev.* **92**, 1457–1470 (1992).
18. A. Mc Nally, R. J. Foster, and T. E. Keyes, "Interfacial supramolecular cyclodextrin-fullerene assemblies: host reorientation and guest stabilization," *Phys. Chem. Chem. Phys.* **11**, 848–856 (2009).
19. C. T. Mallon et al., "Surface-immobilized pyridine-functionalized $\gamma$-cyclodextrin: alkanethiol co-adsorption-induced reorientation," *Langmuir* **23**, 6997–7002 (2007).
20. E. M. M. Del Valle, "Cyclodextrins and their uses: a review," *Process Biochem.* **39**, 1033–1046 (2004).
21. L. Szente and J. Szeman, "Cyclodextrins in analytical chemistry: host–guest type molecular recognition," *Anal. Chem.* **85**, 8024–8030 (2013).
22. K. W. Street, "Cyclodextrin cavity polarity and chromatographic implications," *J. Liq. Chromatogr.* **10**(4), 655–662 (1987).
23. I. Degani and I. Willner, "Lasing of rhodamine B in aqueous solutions containing $\beta$-cyclodextrin," *Chem. Phys. Letter* **104**(5), 496–499 (1984).
24. A. Campion et al., "Electronic energy transfer to metal surfaces: a test of classical image dipole theory at short distances," *Chem. Phys. Lett.* **73**(3), 447–450 (1980).
25. A. Wokaun et al., "Energy transfer in surface enhanced luminescence," *J. Chem. Phys.* **79**, 509–514 (1983).
26. M. Lessard-Viger et al., "FRET enhancement in multilayer core–shell nanoparticles," *Nano Lett.* **9**(8), 3066–3071 (2009).
27. M. J. Snare et al., "The photophysics of rhodamine B," *J. Photochem.* **18**, 335–346 (1982).
28. F. Lopez, P. R. Ojeda, and I. L. Arbeloa, "Flourescence self-quenching of the molecular forms of Rhodamine B in aqueous and ethanolic solutions," *J. Lumin.* **44**, 105–112 (1989).
29. J. R. Lackowicz, "Radiative decay engineering: biophysical and biomedical applications," *Anal. Biochem.* **298**, 1–24 (2001).
30. C. D. Geddes and J. R. Lackowicz, "Editorial: metal-enhanced fluorescence," *J. Fluorescence* **12**(2), 121–129 (2002).
31. A. W. Coleman and I. Nicolis, "Aggregation of cyclodextrins: an explanation of the abnormal solubility of $\beta$-cyclodextrin," *J. Inclusion Phenom. Mol. Recognit. Chem.* **13**, 139–143 (1992).
32. Y. He et al., "Cyclodextrin-based aggregates and characterization by microscopy," *Micron* **39**, 495–516 (2008).
33. G. Gonzalez-Gaitano et al., "The aggregation of cyclodextrins as studied by photon correlation spectroscopy," *J. Inclusion Phenom. Macrocyclic Chem.* **44**, 101–105 (2002).
34. K. Nakashima, J. Duhamel, and M. A. Winnik, "Photophysical processes on a latex surface: electronic energy transfer from rhodamine dyes to malachite green," *J. Phys. Chem.* **97**(41), 10702–10707 (1993).
35. U. Y. Liu, L. Jin, and S. Sun, "Molecular recognition studies on supramolecular systems. 26. Inclusion complexation of natural and amino acid modified $\beta$-cyclodextrins with model substances: ANS and RhB molecules," *Microchem. J.* **64**, 59–65 (2000).

**Alicia V. Veglia** holds a professor position at INFIQC, Institute of Physicochemical Research of Cordoba, Department of Organic Chemistry, National University of Cordoba (UNC), Argentina, and she is a research group leader working within the field of sensors based nanocavities of supramolecular systems, developments of new analytical methods, and molecular modeling.

**Angel Guillermo Bracamonte** holds since 2015, an assistant professor position at UNC and research position at CONICET (Commission of Research in Science, Argentina). During his research career, he held a postdoctoral position at Laval University (2009–2012) and University of Victoria, Canada (2012–2013). He was research visitor at University of Regensburg, Germany (2013) and researcher at the University of Akron, USA (2014). Now, he is research project leader in nanomaterials applied to nanophotonics, biophotonics, and nanomedicine.

# Queries

1. Please review the revised proof carefully to ensure your corrections have been inserted properly and to your satisfaction.

2. If any of your requested changes were not made on this revised proof, it's possible that they were in conflict with the journal's style. For example, author corrections to hyphenation, italics, and capitalization occasionally conflict with journal style. However, if you find that any corrections have been omitted that affect the technical content of your paper, please contact journals@spie.org and also include those corrections in your author response to the proofs.

## Funding Information

The authors have identified the following funders and award numbers, either on the submission form at the time of submission or in the Acknowledgments of the manuscript. Please check this list of funding agencies and make any necessary corrections using the full and official name of the funding organization. You may also wish to edit the Acknowledgments, if needed. This information may be used to help SPIE comply with funding reporting mandates.

- Consejo Nacional de Investigaciones Científicas y Técnicas (National Research Council of Argentine); Funder ID https://doi.org/10.13039/501100002923
- Agencia Nacional de Promoción Científica y Tecnológica (National Agency of Scientific and Technology Promotion of Argentine); Funder ID https://doi.org/10.13039/501100003074
- National University of Cordoba (UNC); Funder ID https://doi.org/10.13039/100010442
- Canadian Grants